Text and references for Nevada Bureau of Mines and Geology Map 135

GEOLOGY OF THE WILLOW CREEK RESERVOIR QUADRANGLE

ELKO COUNTY, NEVADA

by

Alan R. Wallace
U.S. Geological Survey

INTRODUCTION

The Willow Creek Reservoir Quadrangle is in the northeastern Sheep Creek Range in southwestern Elko County, 65 km northeast of Battle Mountain and 20 km east of the small town of Midas (fig. 1). The quadrangle includes the northern half of the Ivanhoe mining district, from which mercury ores were mined intermittently between 1915 and the mid 1970s and gold was produced in the early 1990s. Mapping in the quadrangle is a continuation of a broader study of Tertiary volcanism, extension, and gold-mercury mineralization related to the northern Nevada rift and the Yellowstone hot spot (Wallace, 1991, 1993; Wallace and John, 1998; John and others, 2000). This quadrangle also is along the northwest projection of the Carlin trend, which contains late Eocene gold deposits in Paleozoic sedimentary rocks similar to those that underlie the quadrangle at depth (Teal and Jackson, 1997).

Although many exploration companies have mapped parts of the quadrangle, little has been published on the geology of the study area. The general geology is shown on the Elko County geologic map (Coats, 1987). Bailey and Phoenix (1944) described the mercury deposits in the district, using unpublished mapping and data from J.M. Nelson and R.J. Roberts of the U.S. Geological Survey. During an exploration program for gold in the late 1980s, the geology of parts of the quadrangle were studied and reported by Bartlett and others (1991) and Deng (1991), with an emphasis on the geology of the Hollister gold deposit south of the quadrangle boundary (fig. 1). Preliminary results of the present study were presented in Wallace and John (1998) and in two guidebooks (John and others, 1999; Wallace and John, 2000). Wallace (2003a) shows the geology of the adjacent Willow Creek Reservoir SE Quadrangle. Wallace (2003b) described the geologic and paleogeographic evolution of the district and their effects on mineralization.

The present study shows a complex suite of late Eocene and younger volcanic and volcaniclastic units that unconformably overlies a basement composed of the Ordovician Vinini Formation. The oldest volcanic rocks are ~39 Ma rhyolitic welded tuffs, which were erupted from the Tuscarora Volcanic Field in the Tuscarora Mountains, 10 km to the northeast (fig. 1; Henry and others, 1998), and 37 Ma trachyandesite flows. A thick section of middle Miocene air-fall tuffs and tuffaceous sediments was deposited unconformably on these flows. In the western and southeastern parts of the quadrangle, andesite and rhyolite flows were erupted during sedimentation; in the eastern half of the quadrangle, exogenous rhyolite domes were emplaced near the end of sedimentation. High-angle, northeast- and northwest-striking faults cut and tilted all units. The late Eocene units were tilted approximately 20° prior to deposition of the middle Miocene tuffs and sediments. Mercury- and gold-bearing hydrothermal solutions rose along some of the high-angle faults, forming mercury deposits in massive silica replacement and sinter bodies in the tuffs, disseminated gold deposits in various Miocene rocks, and high-grade gold-silver veins in Paleozoic and deeply buried rhyolitic rocks. Reactivation of many faults in the late Miocene exposed the mercury deposits.

Geochronologic data for the Ivanhoe district and nearby areas are given in table 1. Major-oxide and trace-element compositions of volcanic rocks in the district are given in table 2.

PALEOZOIC ROCKS

Quartzite, chert, and argillite of the Ordovician Vinini Formation (Ov) are the oldest exposed rock units in the quadrangle. They are exposed in the southeastern part of the quadrangle, along the lower part of Ivanhoe Creek, and in a very small area west of Willow Creek Reservoir. Quartzite is the dominant exposed lithology, and it forms prominent blue-gray to light brown outcrops. Argillite may

be present in subequal amounts, especially in the southeastern part of the quadrangle, although it only occurs as small pieces of float. Bartlett and others (1991) reported that both quartzite and argillite were common in drill cores and cuttings. Subordinate to minor exposed lithologies include dark chert, intraformational quartzite breccias, and chert-pebble conglomerate lenses in the quartzite beds. Bartlett and others (1991) encountered minor greenstone during drilling, although none was observed at the surface during this study. Due to the limited outcrops, the only exposed structure in the Vinini is a small, north-northwest-trending antiform in exposures along Ivanhoe Creek.

Quartzarenite (orthoquartzite) has been used to differentiate the Ordovician Valmy Formation from the Vinini, which typically contains more argillite than quartzite (see discussion in Gehrels and others, 2000). Bartlett and others (1991) assigned the Paleozoic rocks in this quadrangle to the Valmy, based on limited fossil data that indicated an Ordovician age. Stratigraphic data and paleontological ages from the Santa Renia Fields Quadrangle to the southeast (fig. 1; Theodore and others, 1998) indicate that the rocks there, which include abundant quartzarenite (orthoquartzite), are part of the Ordovician Vinini Formation. Some of those exposures project northwest to nearby exposures in this quadrangle, and the Paleozoic rocks exposed in this quadrangle thus are assigned to the Vinini Formation. Clearly, though, this assignment is tentative, and detailed biostratigraphic data are needed for the Paleozoic rocks exposed in this quadrangle.

EARLY TERTIARY VOLCANIC ROCKS

The oldest Cenozoic units in the quadrangle are the tuff of Nelson Creek (Tnc) and the tuff of Big Cottonwood Canyon (Tbc). A K-Ar date from this sequence (unit not specified; collected west of Willow Creek Reservoir) produced an age of 32.9±1.1 Ma (recalculated from McKee and others, 1976). However, new $^{40}Ar/^{39}Ar$ dates described below demonstrate a late Eocene age for both tuff units. The tuff of Nelson Creek is the lower of the two pyroclastic units, and it is a single cooling unit with possibly two eruptive units composed of weakly welded, trachydacite to rhyolite ash-flow tuff. It

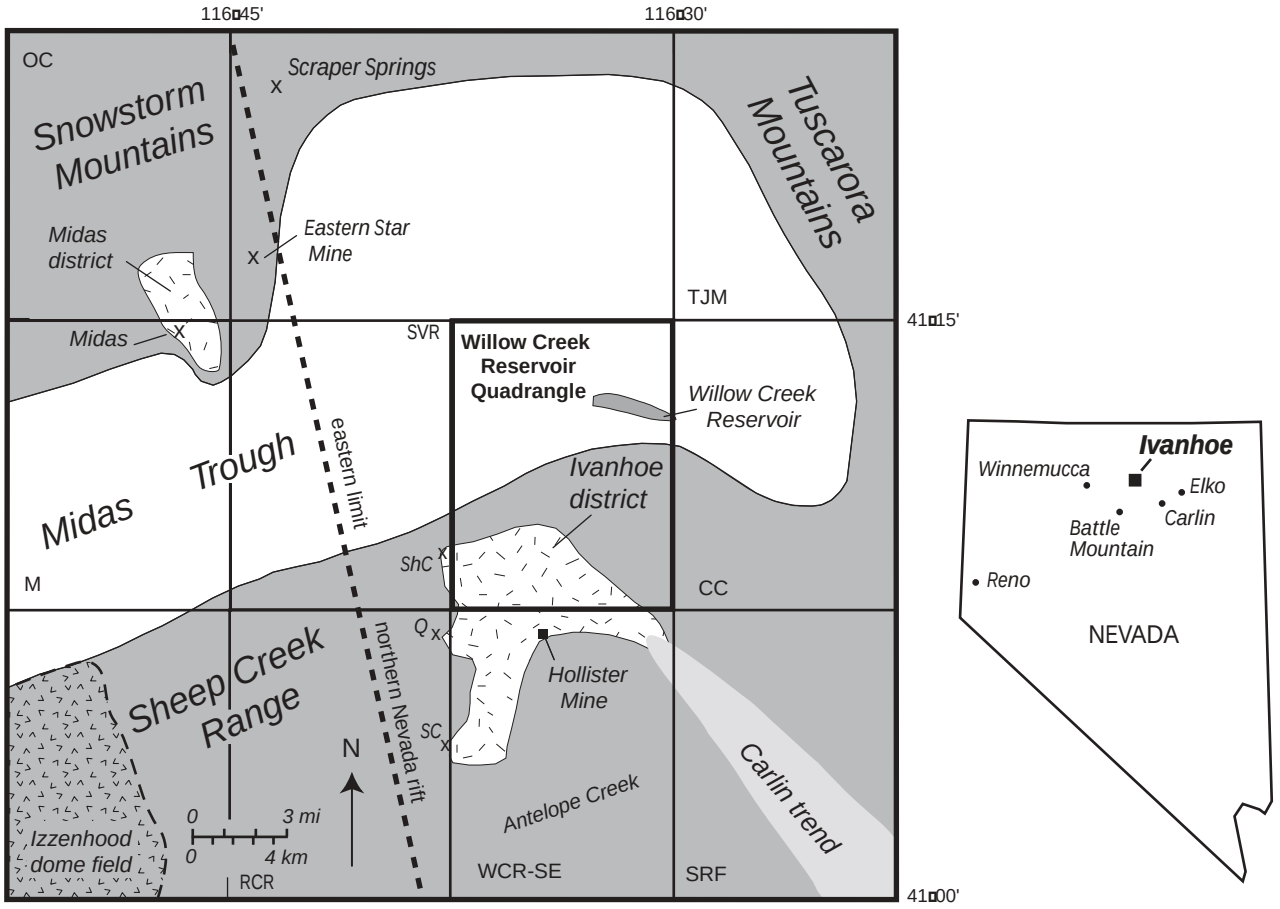

Figure 1. Location of the Ivanhoe mining district, the Willow Creek Reservoir Quadrangle, and geographic features mentioned in text. Geologic quadrangle maps: M, Midas (Wallace, 1993), OC, Oregon Canyon (Wallace, 1993); SRF, Santa Renia Fields (Theodore and others, 1998); TJM, Toe Jam Mountain (Henry and Boden, 1999); WCR-SE, Willow Creek Reservoir SE (Wallace, 2003a). Unmapped quadrangles described in text: CC, China Camp; RCR, Rock Creek Ranch; SVR, Squaw Valley Ranch. Q, Quiver area; ShC, Sheep Corral Mine; SC, Silver Cloud Mine.

overlies the Vinini Formation, with an intervening, poorly exposed paleoregolith composed of red soil and angular fragments of quartzite; no basal vitrophyre is evident in the tuff. The tuff contains abundant rock fragments and pumice; the top of the unit contains large (10–100 cm) pumice clasts that may have rafted to the top of the flow during emplacement of the ignimbrite or may reflect a change in the character of the eruption. Major phenocrysts are plagioclase and biotite, with less-abundant hornblende, quartz, and sanidine (fig. 2). The tuff closely resembles a pumice-rich tuff exposed along Nelson Creek in the Tuscarora Mountains that has a $^{40}Ar/^{39}Ar$ date of 39.42±0.11 Ma (table 1), and the tuff in this quadrangle is correlated with that unit on the basis of stratigraphic position and phenocryst assemblage.

The tuff of Big Cottonwood Canyon overlies the tuff of Nelson Creek, contains few lithic fragments, and is strongly welded. Phenocrysts include smoky quartz, sanidine, and plagioclase in subequal proportions, with minor biotite and no hornblende (fig. 2). The tuff was erupted at 39.22±0.1 Ma, based upon a $^{40}Ar/^{39}Ar$ date on sanidine (table 1). This age is identical to that of the Big Cottonwood Canyon caldera in the Tuscarora Mountains (Henry and Boden, 1998). This age, coupled with the similar compositions and phenocryst assemblages, indicate that the tuff was erupted from that caldera, and it is renamed here from the "tuff of Willow Creek Reservoir" in Wallace and John (1998). The contact with the tuff of Nelson Creek is not exposed, although a lithic accumulation zone is exposed near the base of the tuff of Big Cottonwood Canyon at the Willow Creek Reservoir dam spillway.

Trachyandesite lava flows and tuffs (Tta) overlie the tuff of Big Cottonwood Canyon in the vicinity of the reservoir, but they are thin to absent farther to the west and absent along Ivanhoe Creek. The unit includes upper and lower dark-colored flows with an intervening leucocratic zone of vapor-phase-altered andesitic tuffs and breccias. Biotite from massive, unaltered flows gave a $^{40}Ar/^{39}Ar$ age of 37.23±0.1 Ma (table 1). These flows may be equivalent to other late Eocene intermediate-composition flows near Scraper Springs to the northwest (fig. 1; Wallace and McKee, 1994) and in the Tuscarora Mountains to the east-northeast (Henry and Boden, 1999).

Table 1. Summary of isotopic ages from the Ivanhoe district and vicinity

Rock type/unit	Material dated	Age (Ma)	Method
Ivanhoe area:			
Carlin Formation (Tcas)[a]	sanidine	14.41±0.04-15.10±0.08[1]	$^{40}Ar/^{39}Ar$
Rhyolite porphyry (Trp)	sanidine	14.92±0.05	$^{40}Ar/^{39}Ar$
Craig rhyolite (east) (Tcr)	sanidine	14.99±0.05-15.16±0.05[4]	$^{40}Ar/^{39}Ar$
Air-fall tuff (Ttsu)	——[b]	15.05±0.25[6]	$^{40}Ar/^{39}Ar$, chemistry
Craig rhyolite (west) (Tcr)	sanidine	15.07±0.08-15.17±0.05	$^{40}Ar/^{39}Ar$
Rhyolite of the Velvet area (Trv)	sanidine	15.10±0.05	$^{40}Ar/^{39}Ar$
Hollister Au deposit	adularia	15.10±0.4[2]	K-Ar
Vitric tuff (Tvt)	sanidine	15.10±0.06	$^{40}Ar/^{39}Ar$
Ivanhoe Au vein	adularia	15.19±0.05[8]	$^{40}Ar/^{39}Ar$
Airfall tuff (Ttsl)	plagioclase	≤15.84±0.10	$^{40}Ar/^{39}Ar$
Trachyandesite flow (Tta)	plagioclase	37.23±0.1	$^{40}Ar/^{39}Ar$
Big Cottonwood Can. tuff (Tbc)	sanidine	39.22±0.1	$^{40}Ar/^{39}Ar$
Nelson Creek tuff (Tnc)	sanidine	39.42±0.11[3]	$^{40}Ar/^{39}Ar$
Snowstorm Mountains area:			
Ken Snyder (Midas) Au	adularia	15.14±0.08[5]	$^{40}Ar/^{39}Ar$
Sawtooth dike	adularia	15.19±0.023[9]	$^{40}Ar/^{39}Ar$
Esmeralda Formation (Midas)	sanidine	15.43±0.09[7]	$^{40}Ar/^{39}Ar$

Craig rhyolite (east) dates are from exposures in the Santa Renia Fields Quadrangle (Theodore and others, 1998). Craig rhyolite (west) dates are from two exposures in Rock Creek Ranch Quadrangle: flows ~200 m west of the Willow Creek Reservoir SE Quadrangle and flows overlying the Rock Creek rhyolite in the Quiver area (fig. 1). [a]Carlin Formation of Theodore and others (1998) equivalent to "upper tuff unit" (Ttsu) in Ivanhoe district (see text). [b]Date on upper tuff (Ttsu) based on tephrochronologic correlations (Perkins and others, 1998) and not direct dating of the unit. All data from Wallace and John (1998) and John and others (2000), except for (1) Fleck and others (1998), (2) Bartlett and others (1991; sample from drill core in Hollister deposit), (3) Henry and Boden (1999), (4) R.J. Fleck, written commun. (1999), (5) Leavitt and others (2000; ave. 3 samples), (6) Perkins and others (1998), (7) Leavitt (2001), (8) Peppard (2002), and (9) C. Henry, written commun. (2001). $^{40}Ar/^{39}Ar$ ages were determined at geochronology labs at the U.S. Geological Survey, New Mexico Bureau of Mines and Geology, and the University of Nevada, Las Vegas; these ages were standardized (recalculated) to an age of 27.55 Ma for Fish Canyon Tuff.

Table 2. Chemical analyses of Tertiary rocks from the Ivanhoe mining district, including the Willow Creek Reservoir Quadrangle

Eocene Units:															
Sample ID	**96WC-10**	**96WC-12**	**96WC-14**	**96WC-21**	**96WC-27**	**96WC-28**	**96WC-5**	**96WC-8**	**96WC-13**	**96WC-9**	**96WC-11**	**96WC-15**	**96WC-16**	**96WC-25**	**96WC-30**
Map Unit	**Tbc**	**Tbc**	**Tbc**	**Tbc**	**Tbc**	**Tbc**	**Tnc**	**Tnc**	**Tnc**	**Tta**	**Tta**	**Tta**	**Tta**	**Tta**	**Tta**
Latitude	41-13-55	41-13-45	41-14-13	41-11-18	41-13-36	41-13-35	41-10-13	41-13-51	41-13-45	41-13-58	41-14-02	41-14-48	41-13-50	41-13-37	41-13-37
Longitude	116-34-21	116-33-48	116-33-49	116-36-57	116-33-56	116-32-21	116-36-32	116-34-50	116-33-50	116-34-39	116-34-06	116-33-41	116-33-31	116-32-12	116-32-10
Quadrangle	WCR	WCR	WCR	WCR	WCR	WCR	WCR	WCR	WCR	WCR	WCR	WCR	WCR	WCR	WCR
Major Oxides (percent)															
SiO_2	74.41	75.49	79.95	74.25	74.61	74.29	74.77	74.74	65.89	60.60	60.97	58.67	58.89	63.35	62.82
Al_2O_3	14.34	13.66	10.93	14.80	14.24	14.29	14.44	14.05	18.31	19.77	20.59	20.08	20.39	19.45	20.23
Fe_2O_3	1.64	1.49	1.43	1.12	1.32	1.56	2.12	1.66	3.45	5.03	4.84	6.29	5.51	3.85	3.55
MgO	0.20	0.23	0.19	0.21	0.19	0.23	0.42	0.20	0.68	1.62	0.73	1.16	1.99	0.84	0.74
MnO	0.01	0.01	0.01	0.01	0.02	0.01	0.01	0.01	0.01	0.03	0.01	0.03	0.05	0.03	0.02
CaO	0.90	0.91	1.01	0.89	0.90	1.12	0.62	0.94	3.02	4.95	4.52	4.83	5.26	3.92	4.21
TiO_2	0.09	0.09	0.11	0.10	0.10	0.10	0.10	0.10	0.48	0.62	0.76	0.82	0.74	0.64	0.70
Na_2O	3.55	3.49	2.56	3.57	3.54	3.41	1.85	3.44	3.79	3.94	4.25	4.40	4.21	4.27	4.28
K_2O	4.82	4.53	3.76	5.02	5.05	4.93	5.62	4.67	4.11	3.18	3.00	3.30	2.59	3.28	3.05
P_2O_5	0.04	0.10	0.05	0.04	0.04	0.06	0.07	0.20	0.26	0.26	0.33	0.43	0.37	0.36	0.39
Total	99.20	100.42	98.47	97.83	100.26	98.96	97.56	99.76	98.91	98.50	97.54	97.57	97.44	98.40	98.03
Trace elements (ppm)															
Ag	-0.5	-0.5	-0.5	-0.5	-0.5	-0.5	-0.5	-0.5	-0.5	-0.5	-0.5	-0.5	-0.5	-0.5	-0.5
As	-5	-5	8	-5	-5	-5	-5	-5	-5	-5	-5	-5	18	-5	-5
Ba	736	753	742	676	781	744	787	749	1273	1066	1120	1143	1175	1151	1141
Bi	0.3	0.9	-0.2	0.6	0.8	0.4	-0.2	0.7	0.3	0.4	0.7	1.7	0.6	2.5	0.5
Ce	75	67	53	68	65	69	64	61	75	61	65	61	66	72	72
Co	1.5	0.8	1.3	0.6	0.5	0.6	0.8	1.4	6.2	11.6	10.6	16.6	12.6	8.2	9.6
Cr	4	7	28	3	3	5	-10	6	39	50	22	54	11	14	12
Cs	3.9	3.7	3.1	2.6	3.0	2.7	6.9	3.6	3.1	2.6	1.1	2.1	2.0	1.1	1.5
Cu	-10	-10	-10	-10	-10	-10	-10	-10	-10	-10	-10	11	-10	-10	-10
Dy	7.7	10.0	1.6	2.1	2.1	1.7	2.8	2.1	3.0	3.4	3.4	3.2	4.1	3.7	4.1
Er	3.6	5.2	1.1	1.2	1.4	1.0	1.6	1.3	1.6	1.9	1.7	1.6	2.2	1.9	2.3
Eu	2.5	2.9	0.6	0.6	0.7	0.6	0.8	0.6	1.4	1.4	1.7	1.6	1.7	1.4	1.7
Ga	17	16	13	17	15	16	16	16	21	23	24	24	23	23	24
Gd	11.0	14.0	2.4	3.0	2.7	2.6	3.9	2.9	4.4	4.5	5.1	4.7	6.0	4.9	5.5
Ge	1.0	1.0	-1.0	1.0	1.0	1.0	1.0	1.0	1.0	1.0	1.0	1.0	1.0	1.0	1.0
Hf	3.4	3.6	2.5	3.3	3.2	3.0	4.2	3.4	5.7	4.5	4.4	4.3	4.2	5.4	4.8
Ho	1.2	1.8	0.3	0.4	0.4	0.3	0.5	0.4	0.5	0.6	0.6	0.6	0.7	0.7	0.7
In	-0.2	-0.2	-0.2	-0.2	-0.2	-0.2	-0.2	-0.2	-0.2	-0.2	-0.2	-0.2	-0.2	-0.2	-0.2
La	114	131	45	58	56	61	63	54	67	50	53	49	55	57	55
Lu	0.3	0.5	0.2	0.2	0.2	0.2	0.2	0.2	0.2	0.3	0.2	0.2	0.3	0.2	0.3
Mo	-0.5	-0.5	-0.5	-0.5	-0.5	-0.5	-0.5	-0.5	0.8	-0.5	0.7	-0.5	-0.5	-0.5	-0.5
Nb	10	10	7	10	9	10	10	10	11	10	13	12	12	17	13
Nd	96	104	22	29	28	28	35	27	39	32	38	35	41	39	42
Ni	-10	17	70	-10	-10	-10	-10	-10	90	104	-10	42	-10	-10	-10
Pb	48	40	32	47	50	55	39	49	40	44	46	41	39	30	38
Pr	22.6	23.9	6.0	7.9	7.4	7.8	9.2	7.3	9.8	7.6	9.0	8.1	9.4	9.4	9.4
Rb	145	142	113	146	140	139	158	143	126	93	73	99	100	98	94
Sb	0.6	0.6	0.7	0.6	0.4	0.4	1.0	0.7	0.5	0.6	0.5	0.6	0.5	0.4	0.3
Sm	17.0	19.0	3.4	4.6	4.5	4.3	5.9	4.4	6.4	5.8	7.1	6.2	7.7	6.6	7.5
Sn	1.0	2.0	1.0	2.0	1.0	3.0	-1.0	4.0	-1.0	3.0	1.0	-1.0	2.0	5.0	2.0
Sr	137	136	158	129	141	142	109	133	539	639	751	763	857	685	789
Ta	1.1	1.1	0.8	1.1	0.9	1.0	1.1	1.1	0.9	0.9	1.2	1.1	0.9	1.4	1.1
Tb	1.6	2.1	0.4	0.4	0.4	0.4	0.6	0.4	0.6	0.6	0.7	0.7	0.8	0.7	0.9
Th	28	27	19	29	26	27	27	27	21	15	14	13	10	12	11
Tl	1.0	0.9	0.5	1.1	1.0	1.0	0.9	1.1	0.7	0.7	0.5	0.6	1.6	0.5	0.5
Tm	0.5	0.8	0.2	0.2	0.2	0.2	0.2	0.2	0.2	0.3	0.2	0.2	0.3	0.3	0.3
U	6.2	6.4	5.5	4.9	4.6	3.9	3.9	4.9	3.6	3.5	4.9	3.4	3.0	3.4	3.5
V	-5.0	-5.0	-5.0	-5.0	-5.0	5.0	-5.0	-5.0	61.0	113.0	109.0	124.0	117.0	88.0	105.0
W	1.3	1.2	0.6	1.2	1.1	1.7	2.3	1.4	1.1	1.0	1.0	0.9	0.8	1.1	0.7
Y	34	50	11	14	14	12	17	13	16	20	18	18	24	22	26
Yb	2.5	4.2	1.0	1.2	1.3	1.0	1.5	1.3	1.3	1.6	1.3	1.2	1.7	1.8	2.0
Zn	28	21	26	24	20	23	34	23	54	85	87	88	88	112	90
Zr	112	115	84	101	105	95	129	104	183	146	143	141	145	189	167

Table 2 (*continued*)

Miocene units:																				
Sample ID	**97WC-5**	**97WC-12**	**98WC-3**	**00WC-10**	**97WC-10**	**97WC-11**	**98WC-8**	**98WC-10**	**96WC-3**	**96WC-4**	**96WC-2**	**97WC-1**	**97WC-14**	**97WC-16**	**97WC-7**	**97WC-13**	**96WC-17**	**96WC-18**	**96WC-19**	**96WC-24**
Map Unit	**Ta**	**Ta**	**Ta**	**Ta**	**Tcr**	**Tcr**	**Tcr**	**Tcr**	**Trc**	**Trc**	**Trp**	**Trp**	**Trp**	**Trp**	**Trv**	**Trv**	**Ttsl**	**Tvt**	**Tvt**	**Tvt**
Latitude	41-07-58	41-05-24	41-06-04	41-06-42	41-07-30	41-04-58	41-03-52	41-04-25	41-10-02	41-09-50	41-10-53	41-12-00	41-11-49	41-07-44	41-07-33	41-07-37	41-14-08	41-14-02	41-09-36	41-13-51
Longitude	116-36-16	116-38-07	116-36-48	116-34-35	116-31-43	116-37-50	116-36-27	116-37-00	116-37-35	116-37-32	116-36-08	116-33-30	116-36-40	116-31-05	116-33-34	116-33-32	116-32-57	116-32-39	116-35-20	116-31-31
Quadrangle	WCR	RCR	WCRSE	WCRSE	WCR	RCR	WCRSE	WCRSE	WCR	WCR	WCR	WCR	WCR	WCR	WCR	WCR	WCR	WCR	WCR	WCR
Major Oxides (percent)																				
SiO_2	56.12	56.42	57.67	58.85	76.08	74.22	78.00	75.45	77.11	72.96	74.26	74.96	77.41	79.42	74.06	76.92	66.98	70.92	70.55	70.31
$Al2O_3$	15.23	13.72	13.42	13.86	13.68	12.22	10.89	12.49	13.30	13.86	13.74	14.23	11.62	11.01	13.96	11.51	16.42	15.08	15.61	14.92
Fe_2O_3	11.53	12.57	12.28	10.13	3.65	3.17	1.94	2.16	1.93	3.61	1.60	1.20	1.69	1.49	1.85	1.96	5.52	2.68	3.06	3.48
MgO	2.82	1.89	0.17	2.75	0.08	0.21	0.03	0.03	0.16	0.18	0.18	0.07	0.05	0.70	0.13	0.07	0.05	0.36	0.40	0.46
MnO	0.09	0.19	2.69	0.178	0.01	0.06	0.15	0.17	0.01	0.03	0.01	0.01	0.02	0.02	0.02	0.03	0.07	0.03	0.03	0.04
CaO	5.55	5.81	6.42	6.48	0.29	0.48	0.64	0.96	0.51	0.51	0.72	0.24	0.28	2.14	0.63	0.38	3.05	1.26	1.08	1.83
TiO_2	1.82	2.24	2.75	2.228	0.15	0.23	3.03	2.51	0.26	0.27	0.06	0.04	0.06	0.08	0.11	0.13	0.57	0.30	0.31	0.33
Na_2O	3.51	3.69	1.70	2.86	1.65	4.03	5.08	5.90	1.86	2.96	4.71	4.74	4.29	1.49	3.82	3.88	2.61	2.90	2.38	2.87
K_2O	2.47	2.70	2.10	1.89	4.44	5.35	0.19	0.23	4.81	5.56	4.65	4.47	4.54	3.63	5.32	5.10	3.27	6.40	6.48	5.69
P_2O_5	0.86	0.77	0.27	†0.77	0.01	0.03	0.01	0.02	0.06	0.05	0.06	0.05	0.04	0.01	0.08	0.03	0.10	0.06	0.09	0.06
Total	97.30	98.46	96.94	98.78	96.25	98.75	98.85	95.47	98.39	99.16	97.42	98.80	98.40	94.20	99.36	98.89	89.60	96.74	95.01	95.09
Trace Elements (ppm)																				
Ag	-0.5	-0.5	-0.5	NA	-0.5	-0.5	-0.5	-0.5	-0.5	-0.5	-0.5	-0.5	-0.5	-0.5	-0.5	-0.5	-0.5	-0.5	-0.5	-0.5
As	5.0	9.0	-5.0	NA	-5.0	-5.0	18.9	-5.0	601.0	54.0	-5.0	-5.0	23.0	-5.0	15.0	21.0	22.0	-5.0	-5.0	9.0
Ba	939	1269	1059	1105	1072	1631	653	723	839	1385	15	21	134	3646	148	90	946	1034	977	2452
Bi	1.9	-0.2	0.2	NA	-0.2	-0.2	-0.2	0.2	0.5	3.1	1.0	0.6	2.5	0.6	0.8	0.5	6.9	0.6	0.3	1.2
Ce	81	109	110	86	116	168	180	179	80	104	78	49	80	94	136	173	74	119	118	105
Co	25	22	23	NA	0	0	1	-1	0	1	0	0	0	0	0	0	3	1	2	2
Cr	7.0	5.0	34.7	7.0	5.0	5.0	53.4	23.2	5.0	1.0	2.0	6.0	6.0	42.0	5.0	7.0	7.0	4.0	4.0	5.0
Cs	1.3	4.2	1.8	5.3	2.7	3.8	4.4	4.4	1.6	3.4	9.1	7.6	7.5	5.9	4.7	5.4	2.7	4.1	4.4	6.2
Cu	-10	-10	16	13	-10	-10	18	15	-10	-10	-10	-10	-10	-10	-10	-10	-10	-10	-10	-10
Dy	8.7	8.7	8.7	9.8	6.1	14.0	13.8	13.8	7.3	12.0	22.0	19.0	17.0	15.0	16.0	12.0	8.1	13.0	13.0	12.0
Er	5.1	4.9	5.0	5.2	3.9	9.0	8.9	9.1	4.8	6.8	15.0	13.0	12.0	10.0	10.0	7.9	4.7	7.6	7.8	7.2
Eu	2.4	2.5	2.5	2.7	0.9	1.3	1.1	1.4	0.8	2.0	0.1	0.1	0.1	0.0	0.3	0.3	2.1	1.4	1.4	1.6
Ga	25	22	21	20	21	24	25	24	21	21	31	35	27	21	27	22	23	24	24	22
Gd	10.0	10.0	10.2	10.4	6.5	14.0	17.9	16.2	5.5	13.0	16.0	13.0	12.0	12.0	14.0	12.0	8.8	12.0	13.0	12.0
Ge	2.0	2.0	1.4	NA	2.0	2.0	1.5	1.4	2.0	2.0	2.0	3.0	2.0	2.0	2.0	2.0	1.0	2.0	2.0	1.0
Hf	7.4	7.7	7.1	7.6	9.4	14.0	11.9	12.8	11.0	12.0	9.4	9.1	9.1	7.0	9.3	8.8	8.5	16.0	15.0	15.0
Ho	1.7	1.8	1.7	2.0	1.2	3.0	2.6	2.9	1.6	2.3	4.8	4.1	3.7	3.3	3.3	2.6	1.5	2.5	2.5	2.3
In	-0.2	-0.2	-0.2	NA	-0.2	-0.2	-0.2	-0.2	-0.2	-0.2	-0.2	-0.2	-0.2	-0.2	-0.2	-0.2	-0.2	-0.2	-0.2	-0.2
La	58	50	53	45	55	86	108	96	62	76	51	28	34	40	91	80	57	89	92	89
Lu	0.7	0.7	0.7	0.7	0.8	1.4	1.0	1.3	0.8	1.0	2.3	2.2	1.8	1.5	1.4	1.2	0.7	1.1	1.1	1.1
Mo	1.0	0.7	2.1	NA	2.6	3.1	2.4	3.9	-0.5	1.8	2.1	1.6	2.9	-0.5	2.8	3.0	0.6	2.7	2.4	2.2
Nb	21	25	24	23	32	44	43	45	27	28	46	52	58	42	32	37	18	36	36	32
Nd	54	52	50	50	50	76	92	81	34	67	52	32	38	41	72	66	45	71	73	69
Ni	-10.0	-10.0	67.0	3.0	2.0	5.0	-10.0	13.5	16.0	-10.0	-10.0	-10.0	-10.0	132.0	12.0	0.2	23.0	-10.0	-10.0	17.0
Pb	34	23	38	18	47	52	33	44	53	66	123	95	79	57	86	63	44	53	62	57
Pr	12	13	11	12	14	20	22	19	10	15	12	7	10	11	17	18	10	16	17	16
Rb	84	88	60	65	185	177	186	179	134	171	373	514	444	137	277	311	94	179	191	163
Sb	0.3	0.5	0.3	NA	2.4	1.8	21.2	2.4	2.0	0.6	0.6	0.3	1.8	2.1	0.6	2.4	0.8	0.5	0.9	0.7
Sm	11	11	11	12	10	15	17	16	4	14	15	11	11	11	16	14	9	14	14	14
Sn	3.0	3.0	2.6	NA	4.0	6.0	3.9	5.4	3.0	3.0	16.0	12.0	12.0	12.0	7.0	12.0	3.0	6.0	6.0	6.0
Sr	375	378	372	368	58	59	28	51	89	96	15	8	10	1034	40	15	341	84	73	183
Ta	1.5	1.4	1.4	1.5	2.5	2.4	2.4	2.4	2.1	2.2	6.6	8.3	6.0	4.0	3.7	3.1	1.5	2.8	2.8	2.4
Tb	1.6	1.6	1.3	1.6	1.1	2.4	2.4	2.2	1.3	2.1	3.4	2.9	2.7	2.4	2.8	2.1	1.5	2.2	2.2	2.1
Th	8.2	7.4	7.8	6.0	27.0	18.0	16.7	17.5	17.0	18.0	45.0	50.0	45.0	31.0	35.0	29.0	19.0	27.0	27.0	23.0
Tl	0.4	0.4	0.4	NA	1.2	1.0	0.6	1.9	1.1	1.3	2.0	2.6	1.8	3.6	1.7	1.2	0.7	1.2	1.6	1.1
Tm	0.8	0.7	0.7	0.7	0.7	1.4	1.2	1.3	0.8	1.1	2.6	2.4	2.0	1.7	1.7	1.3	0.7	1.2	1.2	1.1
U	2.7	2.7	2.4	2.5	5.9	4.5	3.5	5.0	4.8	6.0	16.0	14.0	10.0	8.4	9.7	11.0	3.7	6.2	6.6	5.2
V	224	207	232	250	8	-5	9	-5	-5	9	-5	-5	19	6	22	6	1093	-5	10	19
W	0.6	-0.5	1.0	NA	-0.5	-0.5	2.4	1.8	1.9	2.1	5.6	5.1	2.7	2.0	2.6	0.8	0.8	1.5	1.8	1.2
Y	47	51	45	49	27	90	74	82	45	63	120	110	121	109	84	76	43	67	65	64
Yb	4.6	4.8	4.5	4.6	5.0	10.0	6.6	8.5	5.2	6.1	16.0	15.0	14.0	12.0	10.0	8.8	4.4	7.5	7.4	6.6
Zn	170	142	143	142	34	216	130	112	2	161	87	88	58	80	104	67	99	72	81	88
Zr	245	306	286	298	317	536	408	515	364	376	157	134	173	147	217	252	259	464	431	469

Map unit: abbreviations as shown on geologic map and description of map units. Quadrangles (fig. 1): RCR, Rock Creek Ranch; WCR, Willow Creek Reservoir (this map); WCRSE, Willow Creek Reservoir SE (Wallace, 2003a). All analyses by ActLabs, except for 00WC-10 (Geoanalytical Laboratory, Washington State University), major oxide analyses by X-ray fluorescence (XRF); trace element analyses by XRF and ICP-MS. Major oxides are normalized to 100% on a volatile-free basis; total is before normalization. Fe_2O_3 = total Fe, "-" = amount present is less than indicated number; † = amount present is more than indicated number. NA = not analyzed for.

Bartlett and others (1991), based on drilling data and minor exposures in the district, identified a fragmental unit at the Paleozoic-Tertiary contact. This unit is exposed poorly at the Eocene-Paleozoic contact along Ivanhoe Creek, where it includes angular fragments of Vinini quartzite in a red, clay-rich matrix. The unit is exposed in the Hollister Mine, where it underlies the middle Miocene tuffaceous and volcanic units, but it is absent in most places where the Tertiary-Paleozoic contact is exposed. Bartlett and others (1991) proposed a Tertiary pre-volcanic "erosional residuum" origin for the fragmental unit. The angularity of the breccia fragments argues against the deposit being a long-lived surficial deposit, and the unit may include both late Eocene and middle Miocene surficial deposits that developed on top of the Vinini Formation. Similar surficial deposits may have formed above the Eocene units, but the Eocene-Miocene contacts largely are concealed by weathering and mass wasting of the basal Miocene sedimentary rocks.

MIDDLE MIOCENE TUFFACEOUS ROCKS

Middle Miocene volcanic flow units, domes, and tuffaceous rocks underlie the vast majority of the Willow Creek Reservoir Quadrangle. Deposition of the tuffaceous rocks began at about 16.5 Ma and continued to at least 15.05±0.25 Ma and likely to at least 14.92±0.05 Ma (table 1). Various mafic and felsic flows and domes were erupted episodically onto the tuffaceous units during that time, creating an interleaved sequence of flows and tuffs.

The tuffaceous units in the quadrangle represent fairly continuous deposition in both lacustrine and subaerial environments. These rocks are shown on the geologic map as units Ttsu, Tvt, Ttsm, Ttsl, and Tts. As exposed along the north shoreline of Willow Creek Reservoir, more than 200 m of tuffaceous sedimentary rocks and pyroclastic-fall tuffs overlie the late Eocene trachyandesite (Tta). The basal part of the Ttsl section contains air-fall tuffs, some of which contain abundant pumice and accretionary lapilli. Siltstone, sandstone, and conglomerate are most abundant in this part of the section, and clasts of volcanic rocks are similar to rocks exposed in the Tuscarora Mountains to the northeast (fig. 1). The middle third of the Ttsl section was deposited in a lacustrine environment. Ash-rich air-fall tuffs were deposited as finely laminated to massive, weakly reworked tuffaceous sediments. The upper third of the Ttsl section (including both Ttsl and Ttsm) includes massive, strongly reworked tuffs that may have been deposited in shallow lacustrine to subaerial environments. Perkins and others (1998) estimated the age of incipient sedimentation at 16.5±0.5 Ma, and an air-fall tuff in the middle third of the section was dated at ≤15.84±0.10 Ma (table 1). In the Snowstorm Mountains to the west (fig. 1), several ash-flow tuff units (Elko Prince rhyolite; Wallace, 1993) were erupted just before 15.4 Ma (Leavitt, 2001). These tuffs may form part of the massive upper third of the Ttsl section.

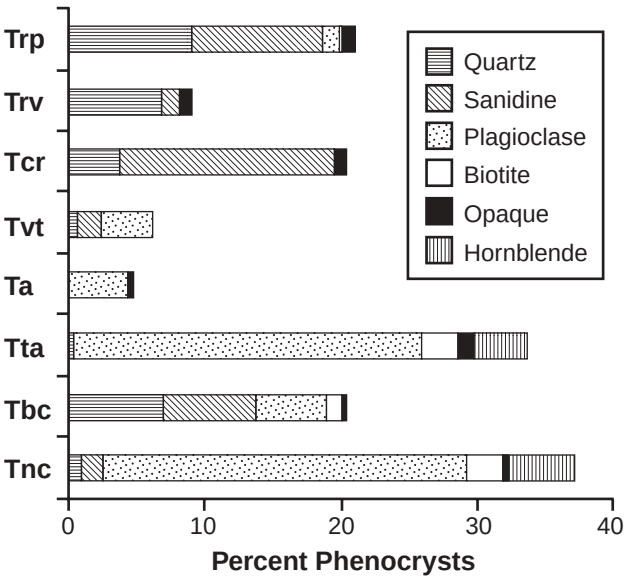

Figure 2. Modal compositions of volcanic rocks in the Willow Creek Reservoir Quadrangle. Unit abbreviations from map unit descriptions.

At 15.10±0.06 Ma (table 1), a vitric tuff (Tvt) was deposited subaerially approximately 200 m above the base of the tuffaceous section. This vitric tuff is characterized by its welded nature and dark-brown to black color speckled with white feldspar phenocrysts, and it forms a distinctive marker bed throughout much of the quadrangle, as well as in areas to the northeast (Henry and Boden, 1999). The thickness of the tuff varies, especially in the northeastern part of the quadrangle, and the basal contact shows a gently undulating paleosurface with local depressions or paleochannels in which the tuff accumulated. Overall, the southward thinning of the unit indicate a northerly, not-too-distant source. A possible source may have been the Owyhee-Humboldt eruptive center in southwesternmost Oregon. That center produced the high-temperature, 15.19±0.04 Ma rhyolite and rhyodacite of the Little Humboldt River (Wallace, 1993; A. Wallace, R. Fleck, unpub. data, 2002). That unit is widespread in and north of the Snowstorm Mountains (fig. 1), and it has a phenocryst assemblage and major oxide chemistry similar to those of the vitric tuff. More proximal eruptive centers in the Snowstorm Mountains are older than the vitric tuff by several hundred thousand years and thus are not possible sources (Wallace, 1993; Leavitt, 2001). Near and south of the south edge of the quadrangle, the vitric tuff is not apparent. By tracing the underlying middle tuff unit (Ttsm) from areas where it clearly is overlain by the vitric tuff to areas where the vitric tuff is not apparent, the post-Ttsm tuffs in the latter areas are more laminated and reworked, indicating deposition in water. Therefore, the vitric tuff likely is part of this waterlain sequence, but deposition in water likely modified the final character of the unit and made it megascopically indistinguishable from the other tuffaceous units.

Tuffaceous sedimentation, largely lacustrine but at times subaerial, continued after emplacement of the vitric tuff to

form the upper tuffaceous sedimentary rocks (Ttsu). Finely laminated beds, with some zones of soft-sediment deformation, attest to the lacustrine conditions. Faulting obscures most of this section of tuffs near the reservoir. However, exposures in the Santa Renia Fields and Willow Creek Reservoir SE Quadrangles to the southeast and south, respectively (fig. 1; Theodore and others, 1998; Wallace, 2003a) reveal more than 400 m of tuffaceous sedimentary rocks that overlie the vitric tuff. Dates in the Santa Renia Fields area range from 14.4 to 15.1 Ma (Fleck and others, 1998), and Theodore and others (1998) correlated the units with the regionally widespread Carlin Formation (Regnier, 1960).

The thicknesses and distributions of the tuffaceous units suggest an early depocenter in the vicinity of Willow Creek Reservoir that gradually filled and, by about 15.1 Ma, expanded into surrounding areas. The lacustrine Esmeralda Formation at Midas (fig. 1), which was deposited between about 15.4 and 15.2 Ma (Wallace, 1993, 2003b; Leavitt and others, 2000), likely is related to this lacustrine system. As noted above, 200 m of sedimentary rocks underlie the vitric tuff at the reservoir. In contrast, only a few tens of meters or less of sediments lie between the vitric tuff and the Vinini basement at the south edge of the quadrangle (Bartlett and others, 1991), and the vitric tuff and all underlying units are absent in the Santa Renia Fields Quadrangle to the southeast (Theodore and others, 1998). In a regional context, therefore, early "Carlin Formation" sedimentation began earlier in the Willow Creek area (~16.5 Ma) than in the Santa Renia Fields Quadrangle (~15.1 Ma) and in the type area near Carlin (Regnier, 1960; C. Henry, written commun., 2002).

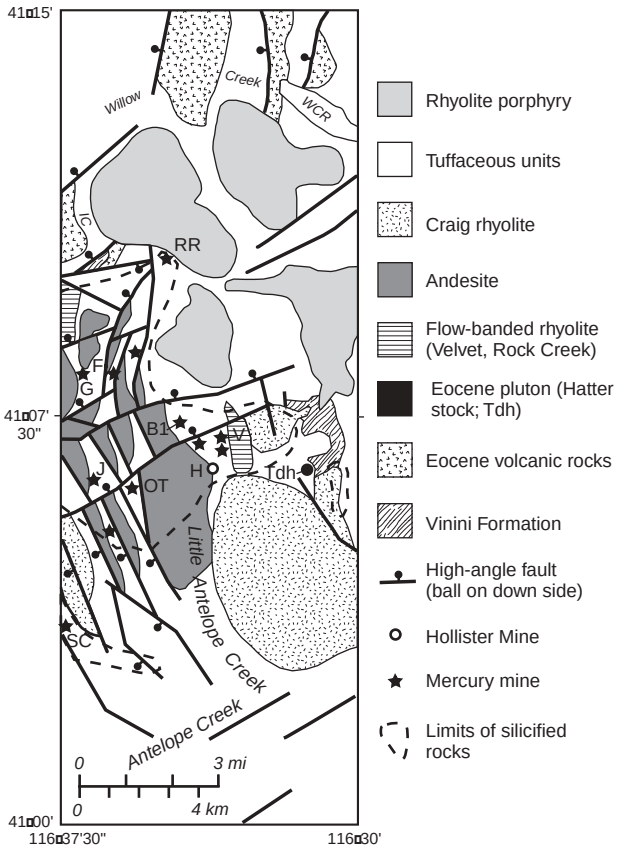

Figure 3. General geology Willow Creek Reservoir (north half of figure) and Willow Creek Reservoir SE (south half) Quadrangles, including the Ivanhoe district. Location shown in figure 1. Mines and prospects: B1, Butte #1; F, Fox; G, Governor; H, Hollister; J, Jackson; OT, Old Timer's; RR, Rimrock; SC, Silver Cloud; V, Velvet. Locations: IC, Ivanhoe Creek; WCR, Willow Creek Reservoir. Geology from this map and Wallace (2003a).

MIDDLE MIOCENE VOLCANIC FLOW UNITS

Rock Creek rhyolite

The Rock Creek rhyolite (Trc; informal name from Bartlett and others, 1991) forms a series of strongly flow-banded and flow-folded crystal-poor rhyolites that was emplaced subaerially during deposition of the lower part of the lower tuff unit (Ttsl). The flows are exposed in the westernmost part of the quadrangle north of the Governor Mine, where they both under- and overlie parts of the lower tuffaceous unit (Ttsl). The flows in this quadrangle form the upper part of a widespread (>50 km^2) and thick (up to 400 m) suite of rhyolite flows that are exposed west and southwest of the quadrangle in the Squaw Valley Ranch and Rock Creek Ranch Quadrangles (fig. 1). There, the rhyolite underlies the middle Miocene Craig rhyolite (Tcr), the various tuffaceous units, and the andesite, and it overlies the Eocene tuffs (A. Wallace, unpub. mapping, 2000–2001).

Both the Rock Creek rhyolite in this area and the June Bell rhyolite at Midas, 15 km to the north (fig. 1; Goldstrand and Schmidt, 2000), are flow-banded, generally aphyric rhyolite flow sequences that occur at about the same stratigraphic level in their respective volcanic sections. Although the Rock Creek rhyolite has not been dated, its presence near the base of the lower tuff unit suggests an age of 15.5–16 Ma. The June Bell rhyolite is older than a 15.54±0.09 Ma tuff higher in the Midas section (Leavitt, 2001).

Andesite

Red to black andesite flows (Ta) are widespread in the southwestern part of the quadrangle. The flows were erupted during deposition of the lower tuff sequence and underlie the vitric tuff (Tvt) by approximately 5–10 m, with an intervening zone of tuffaceous sediments (Ttsm). The absence of hyaloclastic breccias and basal hydration textures, such as those seen at the Hollister Mine (Wallace, 2003a), suggest subaerial volcanism. The andesite pinches out to the east, thinning and ending at a line between the mouth of Ivanhoe Creek and Antelope Spring and extending south through and past the Hollister Mine south of the quadrangle (fig. 3; Bartlett and others, 1991; Wallace, 2003a). The unit

also pinches out to the south and west (Wallace, 2003a; A. Wallace, unpub. mapping, 2001), and the center of the overall area of outcrop is in the northwestern part of the Willow Creek Reservoir SE Quadrangle (fig. 3). As with the vitric tuff, the generally planar top of the unit and the variable total thickness indicate an undulating topography at the time of eruption. Vents for the flows are not exposed and likely were buried by the flows.

Direct dating of the unit proved unsuccessful due to argon loss from the samples. The results from one $^{40}Ar/^{39}Ar$ dating attempt produced a disturbed spectrum that probably resulted from argon loss from glass in the matrix; a probable minimum age of 15.04±0.08 was derived from the highest-temperature step (C. Henry, written commun., 2002). A second dating attempt also was unsuccessful due to significant argon loss (R. Fleck, written commun., 2001). The overlying, 15.10±0.06 Ma vitric tuff unit indicates a somewhat older age for the andesite, and its stratigraphic position just above possible 15.4 Ma units in the lower tuff unit (see earlier discussion) suggests an age of about 15.4 Ma or slightly younger.

Craig rhyolite

Crystal-rich flows units of the Craig rhyolite (Tcr) are exposed in the southeastern part of the quadrangle. The Craig rhyolite is much more extensive in areas to the southeast, southwest, and south, respectively, and it was erupted between 15.17±0.05 and 14.99±0.05 Ma (table 1; Theodore and others, 1998; A. Wallace, unpub. mapping, 2001; Wallace, 2003a). The flow units in this quadrangle underlie the 15.10±0.05 Ma rhyolite of the Velvet area (Trv), indicating that these Craig flow units were erupted early in the Craig rhyolite event. The rhyolite overlies both the upper(?) tuff unit and the Vinini Formation, which were exposed at the time of eruption. The rhyolite contains abundant quartz and locally coarse sanidine phenocrysts; where silicified, both minerals are preserved.

The Craig rhyolite was part of a more widespread rhyolite event that extended from Ivanhoe into the southern Snowstorm Mountains (fig. 1). The Sawtooth dike in the southern Snowstorm Mountains is approximately the same age (15.19±0.023 Ma) as the Craig rhyolite (table 1; Zoback and Thompson, 1978; Wallace, 1993), and it fed an extensive series of rhyolite porphyry flows that chemically and petrographically are similar to those of the Craig rhyolite. Craig rhyolite flows dated at 15.17±0.05 to 15.07±0.08 Ma are exposed in the Silver Cloud Mine and Quiver areas (fig. 1; table 1).

Rhyolite of the Velvet area

The rhyolite of the Velvet area (Trv) is exposed along the south-central border of the quadrangle. The rhyolite extends several kilometers south into the adjacent Willow Creek Reservoir SE Quadrangle (Wallace, 2003a), where it is named for exposures near the Velvet mercury mine. The flows overlie the middle and upper tuff units (Ttsm) to the west and early Craig rhyolite flows to the east, and they were erupted at 15.10±0.05 Ma (table 1). The strong flow banding and flow folding suggest extremely viscous lavas that flowed only a short distance from their sources, and flows in this quadrangle thin to the north. The source vents are not exposed and likely are concealed beneath the main concentration of flow units just south of the quadrangle (Wallace, 2003a).

Rhyolite porphyry

The youngest igneous rocks in the quadrangle are in a series of coalescing, quartz-sanidine-phenocrystic rhyolite flow domes (Trp). The dome east of the mouth of Ivanhoe Creek was emplaced at 14.92±0.05 Ma (table 1). The domes are composed of radially dipping flows that ramp onto adjacent domes, and basal flows extend laterally away from the domes. The relatively uniform basal elevation of the domes and lateral flows indicates a gentle to flat topography at the time of eruption, although local beds of pebble conglomerate directly beneath some domes indicate minor fluvial activity and channels. For the most part, the feeders for these flow domes are buried by their effluent or are difficult to distinguish from the flows. However, a large, north-northwest-striking dike is exposed in the upper Hot Creek drainage in the eastern part of the quadrangle. This orientation is consistent with the west-southwest extension direction in the middle Miocene (Zoback and Thompson, 1978). Several vaguely defined feeder dikes are exposed northwest of this dike. The rhyolite was gas rich and contains locally abundant vesicles and vertical crystal-lined tubes along the margins of the domes. Fluorite and topaz are present in both the vesicles and the groundmass. The domes are similar in form, mineralogy, and composition to 14.84±0.04 Ma domes of the Izzenhood dome field along and south of the Midas trough (fig. 1; Wallace, 1993; John and Wrucke, in press), and in mineralogy and composition to rhyolite porphyry flows in the northwestern Snowstorm Mountains (unit Trpo of Wallace, 1993).

SURFICIAL DEPOSITS

Several late Tertiary to Quaternary unconsolidated sedimentary units are present in the quadrangle. The oldest unit is a terrace gravel (QTg) north of Willow Creek, with small, isolated exposures east of the Rimrock Mine along Ivanhoe Creek and southwest of Big Butte. The gravel north of Willow Creek forms a veneer on a broad terrace that extends to the north and northeast (Henry and Boden, 1999) and dips gently to the west-southwest. Erosion of the underlying tuffaceous sediments (Tts and related units) has redistributed clasts throughout the outcrop area of the tuffaceous units. The subrounded clasts largely are pebble to cobble size, with some as large as 30 cm in diameter. They are composed almost entirely of Paleozoic chert and quartzite, similar to rocks exposed in the Tuscarora

Mountains to the northeast and southeast (fig. 1). This indicates a generally westward transport direction from the source areas, with the fluvial system curling westward around the topographically high rhyolitic dome field, just as Willow Creek does now. Similar east-derived gravel deposits are present on terraces above Antelope Creek in the Santa Renia Fields and Willow Creek Reservoir SE Quadrangles (Theodore and others, 1998; Wallace, 2003a).

The clay-rich nature of the tuffaceous sediments and their ease of erosion, relative to the resistant overlying rhyolite porphyry domes, have generated widespread landslides (Qls) and rhyolite colluvium (Qc) around the flanks of the domes. In places, such as in the basin in the middle of the quadrangle, most exposures of the tuffaceous sediments are obscured by the far-traveled rhyolite colluvium (unit QTcs), although the colluvial veneer is so thin that the underlying sediments are readily apparent.

Alluvial sediments are confined to the Ivanhoe and Willow Creek drainages and small tributaries. Two levels of alluvium are included in unit Qal: narrow deposits of modern sediments along the streams, and finer-grained, somewhat older and thicker deposits that flank both streams. The top of the older deposits in the upper Ivanhoe Creek drainage is at least 6 m above the narrow modern stream bed, and the top of the deposits along Willow Creek is 1 to 2 m above that stream bed. The modern streams have cut steeply into the older alluvial deposits, with little lateral dissection of the older deposits.

STRUCTURAL GEOLOGY

Pre-Miocene structure

Paleozoic tectonism and middle Tertiary deformation affected rocks in and at depth beneath the study area prior to the middle Miocene. Regionally, the Vinini Formation was deposited more than 100 km to the west and was thrust eastward over autochthonous carbonate rocks during the late Devonian-early Mississippian Antler orogeny (Roberts and others, 1958). Deep drilling through the Vinini southeast of the quadrangle indicates the possible presence of these autochthonous units (Tewalt, 1998; Great Basin Gold Ltd, unpub. press release, 2001), and exploration drilling near the Sheep Corral Mine just west of the quadrangle (fig. 1) suggests that related rocks are present at an unspecified depth beneath the Vinini (White Knight Resources Ltd, unpub. press release, 2000). The only pre-Tertiary structure exposed in the quadrangle is a small north-northwest-trending synform in the Vinini along Ivanhoe Creek.

The middle Tertiary deformation included post-37 Ma tilting and the formation of a paleotopographic high. As seen in the Ivanhoe Creek and Willow Creek areas, the late Eocene tuffs and trachyandesite flows were tilted as much as 20° prior to the deposition of the middle Miocene tuffaceous sediments. Evidence near Battle Mountain to the southwest (John and others, 2000) and Emigrant Pass to the southeast (Henry and Faulds, 1999) indicates similar middle Tertiary, pre-Miocene tilting. The faults near Willow Creek Reservoir cut both Eocene and less-tilted overlying Miocene rocks, and the absence of faults that cut and tilted only Eocene rocks indicates that the present faults may have been responsible for both episodes of tilting. Bartlett and others (1991) and more recent exploration drilling (Great Basin Gold Ltd, unpub. data, 2000) show that some high-angle faults in the Hollister area are confined to Paleozoic rocks, but the ages of these faults are unknown. The late Eocene tuffs are absent in the southern part of the quadrangle. Their absence there may be due to middle Tertiary uplift and erosion in that area or to preferential emplacement in a paleovalley in the northern part of the quadrangle.

Bartlett and others (1991) defined a paleotopographic high in the southernmost part of the quadrangle and areas immediately to the south near the Hollister Mine (fig. 1). There, the top of the Paleozoic basement forms an arcuate high with up to 150 m of relief. Bartlett and others (1991), on the basis of drilling conducted throughout the district, related the high to a northwest-trending, pre-Miocene arch through the district. The southward thinning of the middle Miocene tuffaceous sequence suggests the presence of a topographic high during sedimentation. The origin of this high is uncertain, but it may be related in part to the middle Tertiary tilting event.

Miocene structure

The dominant exposed structures in the quadrangle are Miocene high-angle normal faults, the majority of which are best exposed in the northeastern and southwestern parts of the quadrangle. In the northeastern area, the principal strike is north-northeast, and these faults both cut and are cut by west-northwest-striking faults. In the western and southwestern parts of the quadrangle, northeast-, north-, and north-northwest-striking faults are common. The fault sets in these areas are mutually and complexly cross cutting, although northeast-striking faults are younger than north-northwest-striking faults in the Willow Creek Reservoir SE Quadrangle to the south (Wallace, 2003a).

Movement along the faults tilted the Miocene volcanic rocks to the southeast, and few of the faults have more than 100 m of offset. Near Willow Creek Reservoir, faulting repeated the volcanic section at least eight times. Each fault block dips less than the block to the west, with dips decreasing eastward from about 40° to 10°. As much as 25° of tilting took place after deposition of the 15.1 Ma vitric tuff (Tvt) and overlying beds of the upper tuff unit (Ttsu). Although strata in fault blocks throughout much of the quadrangle have dips between 15° and 25°, the dips decrease from steep in the northwest to horizontal in the middle Miocene Carlin Formation along Antelope Creek 20 km to the south (fig. 1; Wallace, 2003a).

Most of the high-angle faulting took place largely after middle Miocene sedimentation. Sedimentary and air-fall tuff units are conformable and their dips are consistent within

fault blocks, indicating that tilting did not precede or accompany sedimentation. Units show no evidence of draping over, thickening across, or ponding against fault-controlled topography, also indicating pre-faulting deposition. In the western part of the quadrangle, tilting took place after the ~15.2 Ma formation of the replacement silica deposits in the middle tuff unit, as those horizons are repeated along with the enclosing tuffaceous and andesite units. However, at the Governor Mine, silicification along a north-striking fault indicates continued hydrothermal activity. In the area between Ivanhoe Creek and Willow Creek Reservoir, the 15.10 Ma vitric tuff was tilted about 20° before the eruption of the overlying 14.92 Ma rhyolite porphyry (Trp). At the Rimrock Mine, tilting took place after silicification of the upper tuff unit. Some high-angle faults cut the rhyolite porphyry domes, and the rhyolite overlies but is not cut by other faults. Thus, various lines of evidence indicate that faulting began at about 15.2 and was most active between 15.2 and 14.92 Ma.

Regionally, northwest-striking Miocene faults are consistent with the middle Miocene west-southwest extension direction (Zoback and Thompson, 1978; Zoback and others, 1994), and northeast-striking faults are related to younger (<8 Ma) northwest-directed extension (Zoback and Thompson, 1978; Wallace, 1991). The faults in this quadrangle grossly fit into that scenario, although the distinct north-northwest and east-northeast fabric produced by those different extension episodes, such as seen in the Snowstorm Mountains to the northwest (fig. 1; Wallace, 1993), is not as clearly expressed in the Willow Creek Reservoir Quadrangle.

The east-northeast-trending Midas trough marks the structural boundary between the Snowstorm Mountains and the Sheep Creek Range (fig. 1), with vertical offsets along bounding faults of as much as 1,000 m. The master fault along the northern margin of the trough splays into at least four lesser faults just west of Midas (fig. 1; Wallace, 1993) and dies as a major structural entity east of Midas. Some northeast-striking faults have been identified in the western Tuscarora Mountains (Henry and Boden, 1999), but their relation to the Midas trough is unknown. The master fault along the south side of the trough extends towards the northwest corner of the Willow Creek Reservoir Quadrangle. Major high-angle, east-northeast-trending normal faults do not project through this quadrangle, and offset along the master fault of the Midas trough may have been distributed over the numerous northeast-striking faults in the Ivanhoe area, similar to the scenario at Midas. These east-northeast-striking faults are nearly absent in the eastern part of the Ivanhoe area, suggesting that the structural zone strongly weakens or dies out here, similar to the northern master fault of the trough.

MIDDLE MIOCENE PALEOGEOGRAPHY

The paleogeographic evolution of the Ivanhoe district is shown in figure 4 (from Wallace, 2003b). The various sedimentary and tuffaceous units indicate both subaerial and subaqueous deposition in an area of low topography that was interrupted by the eruption of the various volcanic flow units. Perkins and others (1998) estimated that tuffaceous sedimentation began near Willow Creek Reservoir as early as 16.5±0.5 Ma, and the basal half of the lower tuffaceous unit had been deposited by about 15.8 Ma (fig. 4a). A topographic high of several hundred meters was present along the southern quadrangle boundary, and Paleozoic rocks in the southeastern part of the quadrangle remained exposed until the eruption of the Craig rhyolite just before 15.1 Ma.

Early sedimentation was both subaqueous and subaerial. Planar, thinly laminated sedimentary rocks indicate subaqueous, lacustrine deposition, and glassy, weakly welded ash and pumice tuffs indicate subaerial deposition. The lakes may have been widespread, extending as far west as Midas by 15.43±0.09 Ma (fig. 1; Wallace, 2000; Leavitt, 2001), and the small amount of coarse clastic material indicates some distance from source highlands or a subdued source topography from which only finer-grained materials were transported. However, pebble conglomerates in the lower part of the section near Willow Creek Reservoir and in the lacustrine sedimentary rocks at Midas (Wallace, 1993) were derived from the northeast and indicate a highland source in that direction.

Rhyolite (Trc) and andesite (Ta) flows were erupted subaerially in the western half of the quadrangle. The Rock Creek rhyolite is interbedded with the basal tuffaceous sediments (Ttsl) and forms an extensive mass west of the quadrangle (A. Wallace, unpub. mapping, 2001). As a result, this area likely was a highland during early sedimentation (fig. 4a). The andesite flowed and pinched out gradually to the east and was deposited on the lower tuff unit; variations in the thickness of the unit suggest a slightly undulating but overall subdued topography (fig. 4b). At the Hollister Mine, the andesite was deposited directly on the Vinini Formation (Ov), and the lower tuffaceous sediments elsewhere in the mine are only a few tens of meters thick. This contrasts with the 200 m of lower tuff section near Willow Creek Reservoir, which likely indicates thinning of this unit against the paleotopographic high.

Sedimentation continued with both lacustrine and subaerial deposition of air-fall tuffs (figs. 4b–d). The middle tuff unit (Ttsm) everywhere was deposited in a quiet lacustrine environment. The vitric tuff largely was deposited subaerially, but it may have been deposited subaqueously in the southernmost part of the quadrangle and in areas to the south (Wallace, 2003a, b), indicating eruption during a drier period, perhaps even seasonal, with scattered small lakes (fig. 4d). Exposures of the base of the upper tuff unit throughout the quadrangle indicate an immediate return to lacustrine conditions (fig. 4e). Major subaqueous soft-sediment slumping deformed lacustrine sediments of the basal upper tuff unit (Ttsu) at Willow Creek Reservoir (fig. 4e). At approximately the same time, debris flows derived from Paleozoic exposures east of the Hollister Mine were deposited at the approximate contact between the middle

and upper tuff units (figs. 4d, e; Wallace, 2003a; Bartlett and others, 1991). High-angle faulting began at about this time (fig. 4e), and seismic shaking may have induced the failures that produced the debris flows and soft-sediment deformation.

Several rhyolites were erupted between about 15.1 and 14.9 Ma, blanketing various parts of the area (figs. 4d–f). The Craig rhyolite (Tcr) and the rhyolite of the Velvet area (Trv) were deposited subaerially on tuffaceous and Paleozoic rocks at about 15.1 Ma, and the rhyolite porphyry domes formed on top of all exposed Miocene units at 14.92±0.05 Ma. In the southeast part of the quadrangle, the Paleozoic rocks remained exposed until the eruption of the Craig rhyolite and rhyolite porphyry domes (Trp). As noted above, faulting had commenced by the time the rhyolite porphyry was erupted, and the flows covered tilted middle Miocene units. Isolated pebble conglomerate beds are exposed at the bases of rhyolite domes in the eastern and southeastern parts of the quadrangle. These beds contain clasts of andesite, which was exposed only to the west, indicating the presence of small streams and an east-flowing drainage pattern just prior to 14.92 Ma (fig. 4f). The formation of the domes undoubtedly interrupted any existing drainage patterns and lakes, including the east-flowing streams. The older gravel deposits (QTg) north of Willow Creek wrap around the north end of the dome field and indicate deflection of that drainage pattern around the domes. Some streams may have flowed through the dome field to deposit gravels such as those near the Rimrock Mine.

MINERAL DEPOSITS

The Willow Creek Reservoir Quadrangle includes the northern half of the Ivanhoe mining district. Mineral deposits in the district include: (1) mercury in extensive near-surface replacement silica zones and more localized sinter deposits, as described by Bailey and Phoenix (1944), principally in the middle tuff unit, (2) disseminated gold in the middle and lower tuff units, the andesite, and the Vinini at the Hollister Mine (Bartlett and others, 1991; Hollister and others, 1992), and (3) recently discovered high-grade gold and silver deposits in the Vinini Formation, Eocene plutonic rocks, and deeply buried Miocene rhyolites (Tewalt, 1998; Great Basin Gold Ltd, unpub. press releases, 1999-2001; various other industry data). The near-surface mercury and disseminated gold deposits are connected vertically (Bartlett and others, 1991; Deng, 1991; Hollister and others, 1992), and drilling data indicate that the high-grade veins beneath these deposits may have been conduits for the more shallow deposits (Great Basin Gold Ltd, unpub. data, 2001); geochronologic data show that all are approximately the same age (table 1). High-grade veins in the Willow Creek Reservoir SE Quadrangle (Wallace, 2003a) are present in Eocene plutonic rocks and nearby Paleozoic rocks. These veins may be related to the Eocene plutonic event, similar to relations to the southeast along the Carlin gold trend (Ressel and others, 2000).

Mercury was discovered in the Ivanhoe area in 1915. Intermittent mining took place until 1943, with brief periods of mining from 1958 to 1973. Total mercury production was 2,180 flasks (LaPointe and others, 1991). The district was explored for porphyry molybdenum deposits in the 1960s and 1970s and for uranium deposits in 1980. Gold exploration began in the late 1970s, and U.S. Steel identified a gold resource 2 km south of the quadrangle at what is now known as the Hollister deposit (fig. 1). Mining at Hollister began in 1990 and continued through 1992, producing 115,000 ounces of gold. Recent (1996–2002) exploration activity in the Hollister area has focused on high-grade gold veins in the Vinini Formation and on deeper targets in Paleozoic rocks that structurally underlie the Vinini. Additional exploration in the district focuses on the Eocene Hatter stock area in the eastern part of the district (fig. 3; Tewalt, 1998; Great Basin Gold Ltd, unpub. data, 2001) and Paleozoic and deeply buried Miocene rhyolite targets elsewhere in the district.

Bailey and Phoenix (1944) provide the most detailed description of the mercury deposits and mining in the Ivanhoe district (fig. 3). Within the quadrangle, the principal mercury deposits include the Governor, Fox, and Rimrock deposits. Other mercury deposits in the district include those at the Velvet, Clementine, Butte #1, Butte #2, Jackson, Old Timer's, Sheep Corral, and Silver Cloud Mines (fig. 3). Most of the silicified zones in the district have been explored by small pits and shallow trenches. The underground parts of the mercury mines were inaccessible during this study, and the deposits could be examined only in limited bulldozer cuts and shallow adits.

Silicification

The most obvious evidence of hydrothermal mineralization in the quadrangle are siliceous sinter and chalcedonic replacement deposits. Sinter deposits, with surface vents, mudcracks, and interbedded outflow breccias, are interbedded locally with sediments of the middle tuff unit. The sinters grade downward into massive to vuggy silicified tuffs. At Hollister, these silicified tuffs contain hypogene kaolinite, jarosite, apatite and alunite that possibly formed at or above the groundwater table during mineralization (Deng, 1991; Hollister and others, 1992). Throughout most of the district, chalcedony replaces a horizon several meters above the base of the middle tuff unit (Ttsm), and linear silicified float and outcrops mark the presence of this interval in areas of poor exposures. Silica also replaced beds in the upper tuff unit (Ttsu) at and east of the Rimrock Mine and west of Big Butte. The replacement deposits are composed of chalcedony that retains the original textures in the host units except in cases of extreme silicification. As exposed in various mine workings, the replacement zones are massive and up to a meter or more thick. More porous zones are common, perhaps indicating volume loss during silicification or late-stage acidic leaching (Hollister and others, 1992; Wallace, 2003b). Silica also replaced

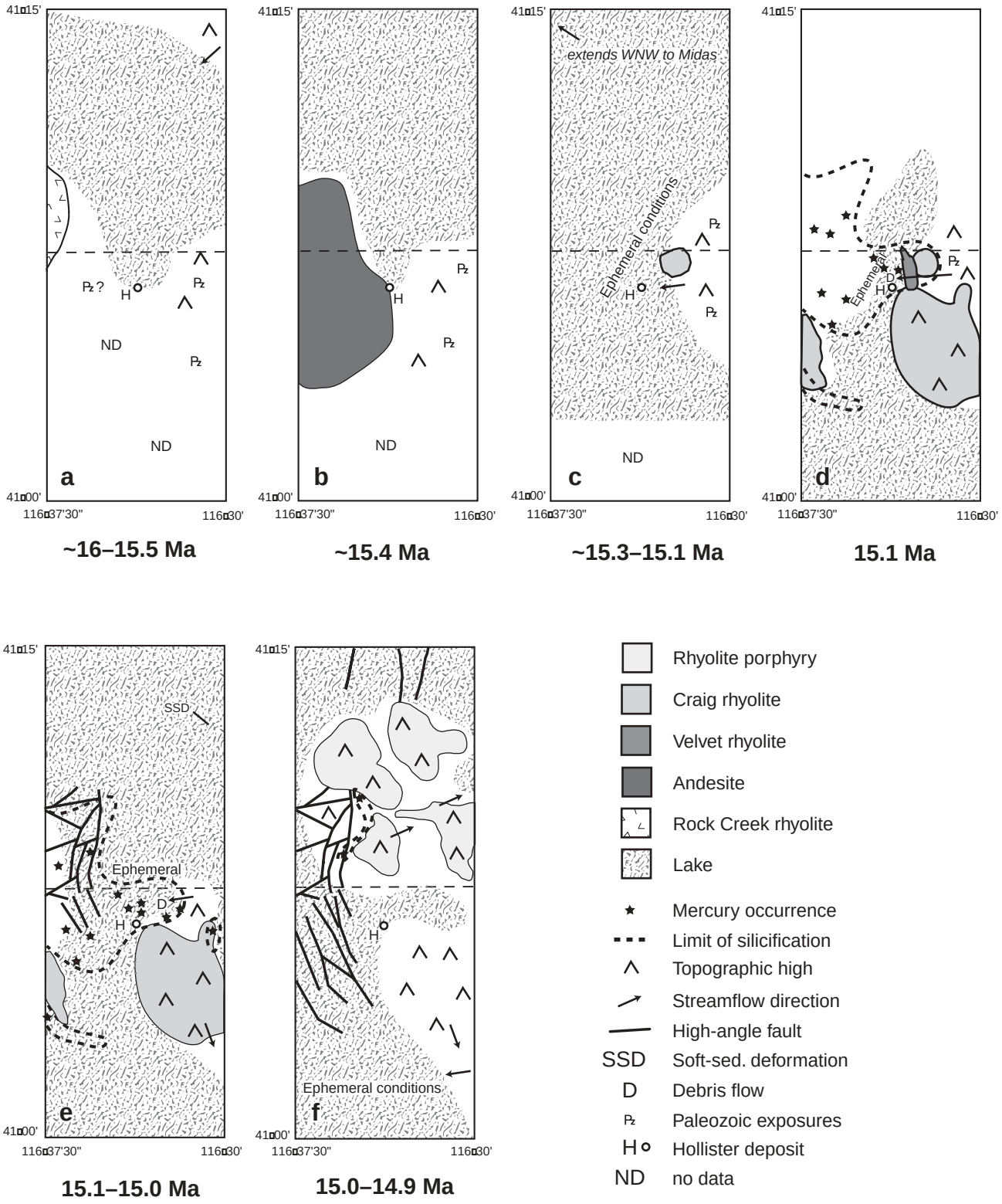

Figure 4. Paleogeographic evolution of the Ivanhoe mining district. Dashed horizontal line is boundary between this quadrangle and Willow Creek Reservoir SE Quadrangle to south (Wallace, 2003a). Hollister Mine (H) shown as reference point in all figures. From Wallace (2003b).

individual thin beds in the tuffs, producing alternating silicified and altered but unsilicified tuffs. In addition to being silicified, the middle tuff unit was bleached and argillically altered near the silicified zones. The andesite and vitric tuff also show evidence of hydrothermal alteration, although fresh rocks commonly both underlie and overlie the replacement deposits in the middle tuff unit, indicating preferential lateral flow of mineralizing fluids along that horizon. At all scales, the silicification front is sharp, with massive silica abutting argillically altered tuff in the same horizon. Vuggy vertical breccia zones with granular chalcedony-supported fragments at the Governor Mine may indicate hydrothermal fluid upwelling and boiling-related brecciation along a high-angle fault, perhaps during faulting.

Mercury was deposited during silica replacement of the middle tuff unit. Cinnabar is the only ore mineral, and it is intergrown with massive chalcedony and forms discrete beds within variably silicified tuff. The cinnabar is black on weathered surfaces and red on fresh faces, reflecting a high chlorine content (McCormack, 2000). As exposed in limited open workings, the cinnabar forms conformable massive to disseminated zones within the altered and silicified tuffs, is intergrown with massive chalcedony, and fills small fractures in silicified tuff. Cinnabar-rich layers are 1–10 cm thick and have sharp contacts with enclosing beds. The cinnabar-bearing horizons preferentially follow thin beds within the host rocks, suggesting possible permeability and porosity influences by the original tuff beds. Other sulfides are not exposed in the mine workings, but pyrite is present in discarded drill cuttings. As seen at the Hollister Mine, the depth of oxidation ranges from ten to more than a hundred meters. Hollister and others (1992) concluded that oxidation was both hypogene and supergene, although fluctuating groundwater table levels during and after mineralization may have been important.

Gold mining has not taken place in this quadrangle. The Hollister gold deposit, 2 km south of the quadrangle boundary (fig. 1), formed several tens of meters beneath silicified tuffs similar to those exposed in this quadrangle. In this quadrangle, several mining companies have explored and drilled for gold in several areas within the district, generally but not exclusively west of Ivanhoe Creek, since the early 1980s. Unpublished exploration data indicate the presence of gold in Miocene, Eocene, and Paleozoic host rocks beneath several of the Miocene-hosted mercury deposits and silicified zones, although the gold grades or depths of intercepts are not publicly available.

Formation of hot-spring-related deposits

The gold and mercury deposits in the Ivanhoe district formed from the same widespread hydrothermal system (Wallace, 2003b). The Hollister deposit formed at 15.1±0.4 Ma (K/Ar date on adularia, table 1; Bartlett and others, 1991), and the high-grade veins beneath the Hollister area formed at 15.19±0.05 Ma ($^{40}Ar/^{39}Ar$ date on adularia, table 1; B. Peppard, C. Hall, written commun., 2001), roughly the age of the nearby rhyolite of the Velvet area (Trv) and early flows of the Craig rhyolite (Tcr). Silicification of the rhyolite of the Velvet area, the Craig rhyolite, and the upper tuff unit, as well as some flows related to the 14.92±0.05 Ma rhyolite porphyry domes, indicates that the district-wide mineralizing process may have spanned 300,000 years, although not necessarily at any one place. Throughout the district, the 15.10±0.06 Ma vitric tuff is weakly to strongly altered in mineralized areas, corroborating these dates on mineralization. This also is the period during which high-angle faulting commenced (figs. 4e, f). The ages for and duration of mineralization are similar to those at the more deeply eroded Midas district, where the principal veins formed at 15.14±0.08 Ma (table 1; Leavitt and others, 2000) and hot-spring mineralization continued for a hundred thousand or more years longer at the nearby Eastern Star Mine (fig. 1; Wallace, 2000, 2003b). The Ivanhoe and Midas districts likely represent the near-surface and somewhat deeper environments of similar epithermal hydrothermal systems (Wallace, 2003b).

As described above, the area of the Ivanhoe district at the time of mineralization had subdued topography, was alternately exposed and covered by shallow lakes (fig. 4), and had a temperate, moist climate (Axelrod, 1956). Thus, meteoric water, either in the lakes or in shallow groundwater, was abundantly available for recirculation in a shallow hot-spring system. Incipient fault activity provided new vertical conduits to flat-lying, unconsolidated, and possibly water-saturated Miocene tuffs and sediments. In the central and southern parts of the district, the widespread Craig rhyolite was erupted at the same time (table 1), and it likely served as the principal heat source for the hydrothermal system. In the northern part of the district, small mercury deposits and silicified zones, such as at the Rimrock Mine and west of Big Butte, formed in the upper tuffaceous unit (Ttsu) adjacent to the 14.92 Ma rhyolite porphyry domes. Silicification and subsequent faulting preceded the dome eruptions, but the high stratigraphic level of the replacement silica indicates an age for silicification that was not much older than dome eruptions. Thus, heat from the ascending but not yet erupted magmas may have produced small hydrothermal systems in those areas. The intercalated and relatively impermeable andesite flow units may have focused fluid flow along its upper surface (fig. 5), or in some way controlled the groundwater table, leading to the almost ubiquitous silicification in tuffs above those flows in this quadrangle. Bartlett and others (1991) argued that the paleotopographic high channeled fluids upward to form the Hollister gold deposit. While that might be the case there, the abundant mercury and replacement silica deposits elsewhere in the district indicate that the high was not an essential element in fluid flow throughout the district.

The stratigraphic positions of the silicified zones in the district shown in figure 5 suggest that the locus of mineralization may have shifted with time, starting in the central part of the district and then moving or expanding laterally south and east (Wallace, 2003b). In the western

half of the district, early silicification (~15.2–15.1 Ma) took place in the middle tuff unit above the andesite and Rock Creek rhyolite (area A, fig. 5). In the Silver Cloud Mine area (area B, fig. 5), massive chalcedony replaced the Craig rhyolite (dated there at 15.07±0.08 Ma) and the overlying upper tuff unit. East of the Hollister area, subsequent silicification above the Vinini, the Craig and 15.10 Ma Velvet rhyolites, and flows of the 14.92 Ma rhyolite porphyry took place after deposition of the upper tuff unit and, locally, the rhyolite porphyry (area C, fig. 5). Similarly, the upper tuff unit in the Rimrock Mine area was silicified shortly before emplacement of the rhyolite porphyry dome (area D, fig. 5). The lake, in all places, was ephemerally present during mineralization (fig. 4).

OTHER GEOLOGIC RESOURCES

Gold, silver, and mercury historically have been the major commodities mined from the Ivanhoe district. Native Americans quarried the chalcedonic replacement bodies in the district for tools and weapons, and evidence of the toolmaking is abundant throughout the area. Volcanic rocks along Willow Creek were quarried in the 20th century for construction of the Willow Creek Reservoir dam. Andesite stripped from above the Hollister orebody was used to construct the haul road from the mine north to the east-west road between Midas and Tuscarora, creating a distinctively red gravel road through this quadrangle. One analysis of an unreworked, water-laid air-fall tuff in the lower tuff unit (Ttsl) west-northwest of Willow Creek Reservoir detected 1093 ppm vanadium. This is higher by one to two orders of magnitude than all the other analyzed rocks in the district, as well as the average vanadium contents of igneous and sedimentary rocks (Krauskopf, 1979). As the lower tuff unit is widespread throughout this quadrangle, additional analyses are needed to determine if parts of this unit contain a vanadium resource.

ACKNOWLEDGMENTS

Chris Henry (Nevada Bureau of Mines and Geology) and Bob Fleck (U.S. Geological Survey) provided essential new $^{40}Ar/^{39}Ar$ dates for the study, and B. Peppard and C. Hall

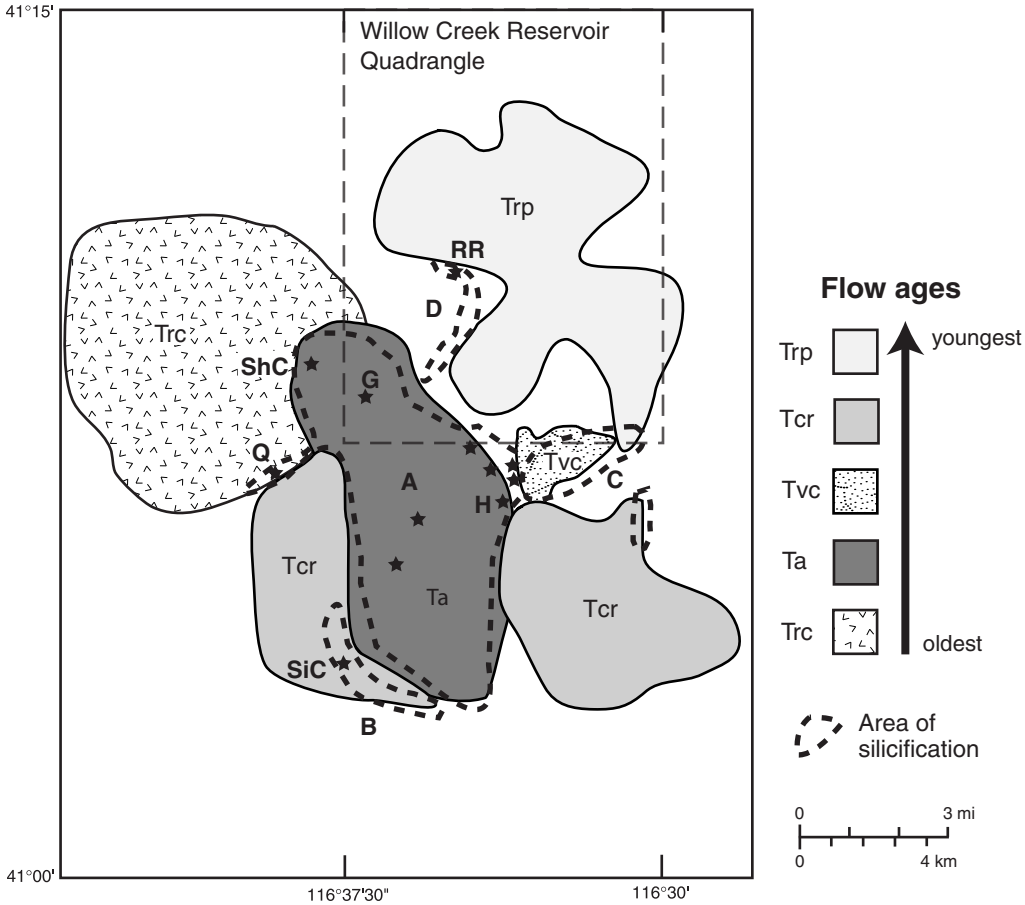

Figure 5. Distribution of major volcanic flow units and areas of silicification (dashed outlines). Willow Creek Reservoir Quadrangle shown with dashed rectangle. Units: Trc, Rock Creek rhyolite; Ta, andesite; Tvc, Velvet and early Craig rhyolites; Tcr, Craig rhyolite; Trp, rhyolite porphyry. Mines and prospects (stars): G, Governor; H, Hollister; Q, Quiver; RR, Rimrock; ShC, Sheep Corral; SiC, Silver Cloud. Letters A–D refer to areas described in text. Modified from Wallace (2003b).

(University of Michigan) shared their new $^{40}Ar/^{39}Ar$ date on the deep veins in the Hollister area. Rosie Moore and Mark Bartlett (Touchstone Resources) first introduced the author to the Ivanhoe area in 1988 and shared ongoing exploration data in the district. Discussions with David John, Chris Henry, Ted Theodore, and Ellie Leavitt provided information on geology in areas surrounding the quadrangle. Industry geologists from several other companies provided surface and drilling information from their exploration work in the quadrangle. Except where cited and with permission, none of their data appear here directly, but their thoughts and ideas helped evaluate the geology in the third dimension. The manuscript benefited from reviews by David John, Dave Boden, and Chris Henry. Robert Chaney, Susan Tingley, Dick Meeuwig, and Jack Hursh of the NBMG provided the manuscript/map preparation and final editing.

REFERENCES

Axelrod, D.I., 1956, Mio-Pliocene floras from west-central Nevada: University of California Publications in Geological Sciences, v. 33, p. 1–322.

Bailey, E.H., and Phoenix, D.A., 1944, Quicksilver deposits in Nevada: Nevada Bureau of Mines and Geology Bulletin 41, 206 p.

Bartlett, M.W., Enders, M.S., and Hruska, D.C., 1991, Geology of the Hollister gold deposit, Ivanhoe district, Elko County, Nevada, *in* Raines, G.L., Lisle, R.E., Schafer, R.W., and Wilkinson, W.H., eds., Geology and ore deposits of the Great Basin: Geological Society of Nevada, Symposium Proceedings, p. 957–978.

Coats, R.R., 1987, Geology of Elko County, Nevada: Nevada Bureau of Mines and Geology Bulletin 101, 112 p.

Deng, Q., 1991, Geology and trace element geochemistry of the Hollister gold deposit, Ivanhoe district, Elko County, Nevada [Ph.D. thesis]: University of Texas-El Paso, 313 p.

Fleck, R.J., Theodore, T.G., Sarna-Wojcicki, and Meyer, C.E., 1998, Age and possible source of air-fall tuffs of the Miocene Carlin Formation, northern Nevada, *in* Tosdal, R.M., ed., Contributions to the gold metallogeny of northern Nevada: U.S. Geological Survey Open-File Report 98-338, p. 176–192.

Gehrels, G.E., Dickinson, W.R., Riley, B.C.D., Finney, S.C., and Smith, M.T., 2000, Detrital zircon geochronology of the Roberts Mountains allochthon, Nevada, *in* Sorgehan, M.J., and Gehrels, G.E., eds., Paleozoic and Triassic paleogeography and tectonics of western Nevada and northern California: Geological Society of America Special Paper 347, p. 19–42.

Goldstrand, P.M., and Schmidt, K.W., 2000, Geology, mineralization, and ore controls at the Ken Snyder gold-silver mine, Elko County, Nevada, *in* Cluer, J.K., Price, J.G., Struhsacker, E.M., Hardyman, R.F., and Morris, C.L., ed., Geology and Ore Deposits 2000: The Great Basin and Beyond, Geological Society of Nevada Symposium Proceedings, May 15–18, 2000, p. 265–287.

Henry, C.D., and Boden, D.R., 1998, Geologic map of the Mount Blitzen Quadrangle, Nevada: Nevada Bureau of Mines and Geology Map 110, scale 1:24,000.

Henry, C.D., and Boden, D.R., 1999, Geologic map of the southern part of the Toe Jam Mountain Quadrangle, Nevada: Nevada Bureau of Mines and Geology Map 117, scale 1:24,000.

Henry, C.D., Boden, D.R., and Castor, S.B., 1998, Geology and mineralization of the Eocene Tuscarora volcanic field, Elko County, Nevada, *in* Tosdal, R.M., ed., Contributions to the gold metallogeny of northern Nevada: U.S. Geological Survey Open-File Report 98-338, p. 279–290.

Henry, C.D., Boden, D.R., and Castor, S.B., 1999, Geologic map of the Tuscarora Quadrangle, Nevada: Nevada Bureau of Mines and Geology Map 116, scale 1:24,000.

Henry, C.D., and Faulds, J.E., 1999, Geologic map of the Emigrant Pass Quadrangle, Nevada: Nevada Bureau of Mines and Geology Open-File Report 99-9, scale 1:24,000.

Hollister, V., Hruska, D., and Moore, R., 1992, A mine-exposed hot spring deposit and related epithermal gold resource: Economic Geology, v. 87, p. 421–424.

John, D.A., and Wrucke, C.T., in press, Geologic map of the Izzenhood Spring Quadrangle, Lander County, Nevada: U.S. Geological Survey Miscellaneous Investigations Series Map I-2668, scale 1:24,000.

John, D.A., Garside, L.J., and Wallace, A.R., 1999, Magmatic and tectonic setting of late Cenozoic epithermal gold-silver deposits in northern Nevada, with an emphasis on the Pah Rah and Virginia Ranges and the northern Nevada rift, *in* Kizis, J.A., Jr., ed., Low-sulfidation gold deposits in northern Nevada: Geological Society of Nevada, 1999 Spring Field Trip Guidebook, Special Publication No. 29, p. 64–158.

John, D.A., Wallace, A.R., Ponce, D.A., Fleck, R.J., and Conrad, J.E., 2000, New perspectives on the geology and origin of the northern Nevada rift, *in* Cluer, J.K., Price, J.G., Struhsacker, E.M., Hardyman, R.F., and Morris, C.L., eds., Geology and Ore Deposits 2000: The Great Basin and Beyond: Geological Society of Nevada Symposium Proceedings, May 15–18, 2000, p. 127–154.

Krauskopf, K.B., 1979, Introduction to Geochemistry (2nd ed.). McGraw-Hill, New York, 617 p.

LaPointe, D.D., Tingley, J.V., and Jones, R.B., 1991, Mineral resources of Elko County, Nevada: Nevada Bureau of Mines and Geology Bulletin 106, 236 p.

Leavitt, E.D., 2001, Hydrothermal alteration and geochronology of the Colorado Grande vein, Ken Snyder mine, Elko County, Nevada: Ralph J. Roberts Center for Research in Economic Geology, Annual Research Meeting 2000, Program and Reports, Feb. 7–8, 2001, 15 p.

Leavitt, E.D., Goldstrand, P., Schmidt, K., Wallace, A.R., Spell, T., and Arehart, G.B., 2000, Geochronology of the Midas gold-silver deposit and its relationship to volcanism and mineralization along the northern Nevada

rift, *in* Wallace, A.R., and John, D.A., eds., Volcanic history, structure, and mineral deposits of the north-central northern Nevada rift: Field Trip Guidebook No. 8, Geological Society of Nevada Symposium 2000, The Great Basin and Beyond, p. 157–162.

McCormack, J.K., 2000, The darkening of cinnabar in sunlight: Mineralium Deposita, v. 35, p. 796–798.

McKee, E.H., Tarshis, A.L., and Marvin, R.F., 1976, Summary of radiometric ages of Tertiary volcanic and selected plutonic rocks in Nevada. Part V: Northeastern Nevada: Isochron/West, no. 16, p. 15–27.

Peppard, B., 2002, Geology and geochemistry of the Ivanhoe vein system, Elko County, Nevada [M.S. thesis]: University of Michigan, Ann Arbor, 49 p.

Perkins, M.E., Brown, F.H., Nash, W.P., McIntosh, W., and Williams, S.K., 1998, Sequence, age, and source of silicic fallout tuffs in middle to late Miocene basins of the northern Basin and Range province: Geological Society of America Bulletin, v. 110, p. 344–360.

Regnier, J., 1960, Cenozoic geology in the vicinity of Carlin, Nevada: Geological Society of America Bulletin, v. 71, p. 1191–1199.

Ressel, M.W., Noble, D.C., Henry, C.D., and Trudel, W.S., 2000, Dike-hosted ores of the Beast deposit and the importance of Eocene magmatism in gold mineralization of the Carlin trend, Nevada: Economic Geology, v. 95, p. 1417–1444.

Roberts, R.J., Hotz, P.E., Gilluly, J., and Ferguson, H.G., 1958, Paleozoic rocks of north-central Nevada: American Association of Petroleum Geologists Bulletin, v. 81, p. 2045–2060.

Teal, L., and Jackson, M., 1997, Geologic overview of the Carlin trend gold deposits and descriptions of recent deep discoveries, *in* Vikre, P., Thompson, T.B., Bettles, K., Christensen, O., Parratt, R., eds., Carlin-type gold deposits field conference: Society of Economic Geologists Guidebook Series, v. 28, p. 3–37.

Tewalt, N.A., 1998, Subtle surface expression of high grade veins at the Ivanhoe project: 1998 Fall Field Trip Guidebook, Geological Society of Nevada, Special Publication No. 28, p. 149–161.

Theodore, T.G., Armstrong, A.K., Harris, A.G., Stevens, C.H., and Tosdal, R.M., 1998, Geology of the northern terminus of the Carlin trend, Nevada: Links between crustal shortening during the Late Paleozoic Humboldt orogeny and northeast-striking faults, *in* Tosdal, R.M., ed., Contributions to the gold metallogeny of northern Nevada: U.S. Geological Survey Open-File Report 98-338, p. 69–105.

Wallace, A.R., 1991, Effect of late Miocene extension on the exposure of gold deposits in north-central Nevada, *in* Raines, G.L., Lisle, R.E., Schafer, R.W., and Wilkinson, W.H., eds., Geology and ore deposits of the Great Basin: Geological Society of Nevada, Symposium Proceedings, p. 179–183.

Wallace, A.R., 1993, Geologic map of the Snowstorm Mountains and vicinity, Elko and Humboldt Counties, Nevada: U.S. Geological Survey Miscellaneous Investigations Series Map I-2394, scale 1:50,000.

Wallace, A.R., 2000, Tertiary geology of the Ivanhoe mining district, *in* Wallace, A.R., and John, D.A., eds., Volcanic history, structure, and mineral deposits of the north-central northern Nevada rift: Field Trip Guidebook No. 8, Geological Society of Nevada Symposium 2000, The Great Basin and Beyond, p. 135–145.

Wallace, A.R., 2003a, Geologic map of the Willow Creek Reservoir SE Quadrangle, Elko Counties, Nevada: Nevada Bureau of Mines and Geology Map 136, scale 1:24,000.

Wallace, A.R., 2003b, Geology of the Ivanhoe Hg-Au district, northern Nevada: Influence of Miocene volcanism, lakes, and active faulting on epithermal mineralization: Economic Geology, v. 98.

Wallace, A.R., and John, D.A., 1998, New studies of Tertiary volcanic rocks and mineral deposits, northern Nevada rift, *in* Tosdal, R.M., ed., Contributions to the gold metallogeny of northern Nevada: U.S. Geological Survey Open-File Report 98-338, p. 264–278.

Wallace, A.R., and John, D.A., eds., 2000, Volcanic history, structure, and mineral deposits of the north-central northern Nevada rift: Field Trip Guidebook No. 8, Geological Society of Nevada Symposium 2000, The Great Basin and Beyond, 175 p.

Wallace, A.R., and McKee, E.H., 1994, Implications of Eocene through Miocene ages for volcanic rocks, Snowstorm Mountains and vicinity, northern Nevada: U.S. Geological Survey Bulletin 2081, p. 13–18 p.

Zoback, M.L., and Thompson, G.A., 1978, Basin and Range rifting in northern Nevada: clues from a mid-Miocene rift and its subsequent offsets: Geology, v. 6, p. 111–116.

Zoback, M.L., McKee, E.H., Blakely, R.J., and Thompson, G.A., 1994, The northern Nevada rift—Regional tectonomagmatic relations and middle Miocene stress direction: Geological Society of America Bulletin, v. 106, p. 371–382.